

Change of Bi₂Te₃ band structure under hydrostatic compression

V. V. Sologub, M. L. Shubnikov, E. S. Itskevich, L. M. Kashirskaya, R. V. Parfen'ev, and A. D. Goletskaya

A. F. Ioffe Physicotechnical Institute, USSR Academy of Sciences and Institute of High-Pressure Physics, USSR Academy of Sciences

(Submitted 16 June 1980)

Zh. Eksp. Teor. Fiz. 79, 2374–2380 (December 1980)

The effect of hydrostatic compression on the Shubnikov–de Haas effect in *n*- and *p*-Bi₂Te₃ samples with different degrees of filling of the valence and conduction bands is investigated. A flow of carriers between nonequivalent extrema in the band, under the influence of the pressure, is observed. It is shown that the energy gap between the extrema increases with pressure in the conduction band, and decreases in the valence band. The latter leads at a pressure $P = 7$ kbar to an electronic transition wherein the absolute extremum of the valence band is changed.

PACS numbers: 71.25.Tn

Measurements of the Shubnikov–de Haas (SH) oscillations, whose period is determined in the general case by the extremal intersection of the Fermi surface with a plane perpendicular to the magnetic field,

$$\Delta\left(\frac{1}{H}\right) = \frac{2\pi e}{\hbar c S_{\text{extr}}}, \quad (1)$$

performed under normal pressure,^{1,2} have shown that the Fermi surfaces of electrons and holes in a narrow-band strongly anisotropic (layered) semiconducting compound Bi₂Te₃ become much more complicated when the Fermi energy exceeds a threshold value $E_p = 15$ – 20 MeV in the valence band and $E_n = 20$ – 30 MeV in the conduction band.^{1–4} The values of the corresponding hole and electron threshold densities p^* and n^* are $(3$ – $5) \times 10^{18}$ cm⁻³.

The present paper is devoted to an investigation of the SH effect in bismuth telluride under hydrostatic compression, with an aim at determining the baric dependences of the low values of the threshold energies and of the possible restructuring of the carrier energy spectrum in Bi₂Te₃.

EXPERIMENTAL PROCEDURE

The SH oscillations in Bi₂Te₃ single crystals were measured at helium temperatures in magnetic fields up to 70 kOe. At normal pressure, we investigated samples with different filling of the valence and conduction bands: p_R from 1.6×10^{18} to 2.4×10^{19} cm⁻³, and n_R from 1.6×10^{18} to 2.1×10^{19} cm⁻³ (see Table I). The carrier densities p_R and n_R were determined from the Hall coefficients measured in maximum magnetic fields, $R_{123} = R_3$ and $R_{231} = R_1$, using the formula

$$n_R = 2/ec(R_1 + R_3).$$

In samples of both types, with carrier densities above the threshold values, we investigated the influence of hydrostatic compression up to $P = 12$ kbar on the Hall coefficient and on the SH oscillations in the transverse magnetoresistance. The dependences of the investigated signals on the magnetic field were plotted with an *x*-*y* recorder. To separate the oscillating parts we subtracted the Hall-pickup signal linear in the magnetic field from the investigated signals, followed by ampli-

fication. The procedure used to produce and record the high hydrostatic pressure is described in Refs. 5 and 6. The pressure was determined from the superconducting transition temperature of tin. The pressure-transmitting medium was a mixture of 60% pentane and 40% oil or the PES-5 polyethylenesiloxane liquid. The hydrostatic pressure was produced at room temperature, after which the chamber was cooled for two hours to helium temperature. It is known that slow cooling of an isotropic mixture does not disturb significantly the hydrostatic character of the pressure at the center of the chamber channel,⁵ as is confirmed also by the distinct picture of the SH oscillations under pressure.

EXPERIMENTAL RESULTS FOR *p*-Bi₂Te₃

According to the six-ellipsoid Drabble-Wolfe (DW) model proposed⁷ for Bi₂Te₃, all six ellipsoids have at $H \parallel C_3$ (H is the magnetic field and C_3 is the crystal trigonal axis) equal extremal sections and the oscillations should have the same period. In samples with hole density above critical, $p_R > p^*$, we observed besides the principal period Δ_3^I also a large second period $\Delta_3^{II} > \Delta_3^I$, i.e., at $\xi > E_p$ (ξ is the chemical potential of the carriers) the hole Fermi surface has two external sections of unequal size: principal S_3^I and additional S_3^{II} . These results are treated as the appearance of additional extrema located 15–20 MeV below the top of the

TABLE I. Principal parameter of the investigated samples at $T = 4.2$ K.

N	$p_R, n_R,$ 10^{18} cm ⁻³	$\sigma_n,$ $10^3 \Omega^{-1}$ cm ⁻¹	$\Delta_3^I,$ 10^{-6} Oe ⁻¹	$\Delta_3^{II},$ 10^{-6} Oe ⁻¹	p_I, n_I 10^{18} cm ⁻³	$\frac{m_3^I}{m_0}$	$\frac{m_{\text{min}}^I}{m_0}$
1p	1.6	18	9.5	—	1.6	0.09±0.005	0.069±0.005
2p	3.0	17	6.05	—	3.1	0.105±0.005	0.072±0.005
3p	7.1	20	4.3	22±2	5.2	0.113±0.005	0.081±0.005
4p	10.9	19	3.64	16.5±1	6.7	—	—
5p	11.6	19	3.55	16.0±1	7.0	—	—
6p	12.0	19	3.5	15.5±1	7.1	—	—
7p	17.0	17	2.85	8.8±0.5	9.7	—	—
8p	24.0	15	2.35	6.2±0.5	13.0	—	—
9n	1.6	20	12.1	—	1.13	—	—
10n	3.15	10.6	6.2	—	3.1	0.077±0.005	—
11n	11.4	13.2	4.05	—	5.8	—	—
12n	19	34	3.2	—	8.3	—	—
13n	21	36	3.06	—	8.9	—	—

* m_{min}^I is the cyclotron mass in the direction of the elongation of the principal valleys in the mirror plane.

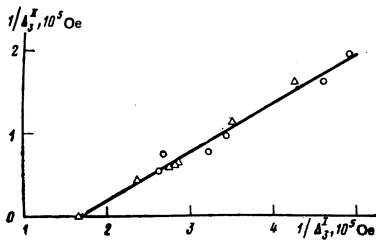


FIG. 1. Reciprocal second oscillation period $1/\Delta_3^{\text{II}}$ vs the reciprocal principal period $1/\Delta_3^{\text{I}}$ for $p\text{-Bi}_2\text{Te}_3$ at $\text{H}\parallel\text{C}_3$ and $T = 4.2$ K. Triangles—present data, circles—data of Ref. 3.

ground band.^{2,3} The filling of the valence band begins with the principal valleys (index I), and at $p_R > p^*$ there appear the sections of the additional valleys (index II).

Figure 1 shows the relation between the quantities $1/\Delta_3^{\text{II}}$ and $1/\Delta_3^{\text{I}}$, obtained for Bi_2Te_3 samples with $p_R > p^*$ at $P = 1$ bar. The experimental points fit well a straight line, thus indicating that the principal and additional sections increase proportionally with increasing hole density.

The chemical potential ζ is connected with the oscillation period by the relation

$$\zeta = \frac{e\hbar}{mc} \left[\Delta \left(\frac{1}{H} \right) \right]^{-1}, \quad (2)$$

where m is the cyclotron mass at the Fermi level. Substitution in (2) of the quantity $(1/\Delta_3^{\text{I}})^* = (1.65 \pm 0.05) \times 10^5 \text{ Oe}^{-1}$, which corresponds to the intercept of the straight line on the abscissa axis (Fig. 1) and of the values $m_3^{\text{I}} = (0.105 \pm 0.05)m_0$, determined from the temperature dependence of the SH oscillation amplitude at $\text{H}\parallel\text{C}_3$ on sample No. $2p$ with period $\Delta_3^{\text{I}} \approx (\Delta_3^{\text{I}})^*$, leads to a chemical potential $\zeta = E_p = 18.0 \pm 1.5 \text{ MeV}$.

Since expression (2) for the holes in the additional valleys determines the value of the chemical potential ζ^{II} reckoned from the E_p level, we can write

$$E_p = \frac{e\hbar}{m_3^{\text{I}}c} (\Delta_3^{\text{I}})^{-1} = \frac{e\hbar}{m_3^{\text{II}}c} (\Delta_3^{\text{II}})^{-1}. \quad (3)$$

From (3) and from the data of Fig. 1 it follows that at $\text{H}\parallel\text{C}_3$ the ratio of the cyclotron masses of the holes in the principal and additional valleys remains the same when the valence band is filled, and is equal to $m_3^{\text{I}}/m_3^{\text{II}} = 1.8$. This value will be used below in the analysis of the experimental data obtained under pressure.

We investigated under hydrostatic compression sample No. $2p$ ($p_R < p^*$) and sample No. $6p$ ($p_R > p^*$), in which both the principal and the additional periods of the SH oscillations were observed at normal pressure.

Figure 2 shows the baric dependences of the reciprocal oscillation periods, measured for sample No. $2p$ at three nearly mutually perpendicular directions of the magnetic field. It is seen that the extremal sections of the Fermi surface are less than half their values at normal pressure, corresponding to an almost threefold decrease of the volume of the principal valleys and to an equal decrease of the hole density in them. Inasmuch as in the same pressure interval the total hole density in the sample remains unchanged (accurate to 10%), as

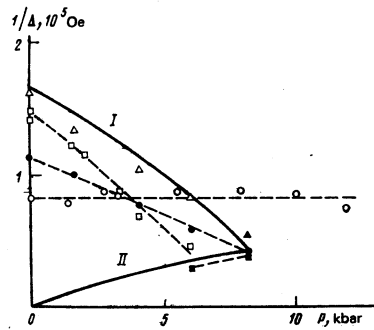


FIG. 2. Reciprocal periods of SH oscillations vs. pressure in $p\text{-}$ and $n\text{-Bi}_2\text{Te}_3$ samples with carrier density below critical. The Roman numbers I and II label data pertaining to the principal and additional parts of the Fermi surface. Solid lines—calculation for sample $2p$ at $\text{H}\parallel\text{C}_3$, dashed—experimental average. Sample No. $2p$: \bullet $1/\Delta_m^{\text{I}}$, magnetic field in mirror plane at an angle 14° to the binary axis (in the elongation direction of the principal valleys), \square $1/\Delta_2^{\text{I}}$, \blacksquare $1/\Delta_2^{\text{II}}$, $\text{H}\parallel\text{C}_2$; \triangle $1/\Delta_3^{\text{I}}$; \blacktriangle $1/\Delta_3^{\text{II}}$, $\text{H}\parallel\text{C}_3$. Sample No. $9n$: \circ $1/\Delta_3^{\text{I}}$, $\text{H}\parallel\text{C}_3$.

follows from the weak dependence of R_3 on the pressure, it is natural to assume that with increasing pressure the threshold energy E_p decreases and the holes flow over from the principal to the additional valleys.

From this point of view, the break on the plot of $1/\Delta_2$ against $P(\text{H}\parallel\text{C}_2)$ in Fig. 2 becomes understandable. Up to $P = 6$ kbar the magnetoresistance oscillations are due to the holes of the principal valleys. Their outflow decreases the density with increasing pressure, thereby decreasing $1/\Delta_2^{\text{I}}$. Above $P = 6$ kbar, the observed oscillations are due to the holes from the additional cavities, the hole density increases with pressure, and $1/\Delta_2^{\text{II}}$ also increases. At $P = 6.0$ kbar the holes of both type make comparable contribution to the SH effect and the magnetoresistance oscillates with two periods, as in the sample with $p_R > p^*$ at normal pressure.

The oscillations in sample No. $6p$ had oscillations with two periods at $\text{H}\parallel\text{C}_3$ in the entire range of investigated pressures. The baric dependences of $1/\Delta_3^{\text{I}}$ and $1/\Delta_3^{\text{II}}$ are shown in Fig. 3, which illustrates clearly the flow-over effect: $1/\Delta_3^{\text{I}}$ decreases and $1/\Delta_3^{\text{II}}$ increases with pressure.

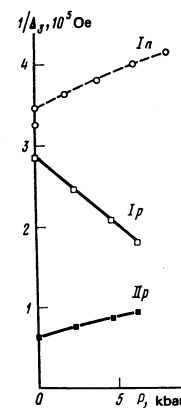


FIG. 3. Dependence of reciprocal magnetoresistance-oscillation periods on pressure at $\text{H}\parallel\text{C}_3$. Sample No. $6p$: I_p principal period, II_p second period; sample No. $10n$: I_n principal period.

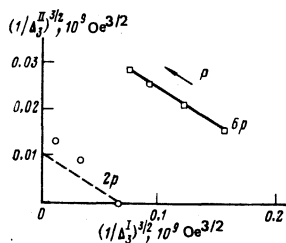


FIG. 4. Relation between the quantities $(1/\Delta_3^I)^{3/2}$ and $(1/\Delta_3^{II})^{3/2}$ in samples 2p and 6p at various pressures. Dashed—calculated relation for sample No. 2p with the parameters determined for parameter 6p; the arrow marked P shows the direction of increasing pressure.

DISCUSSION OF RESULTS FOR ρ -Bi₂Te₃

For a quantitative analysis of the presented experimental data we assume that the baric dependences of the oscillation periods, as well as the Hall coefficient R_3 in samples 2p and 6p are due mainly to the flow-over effect and that the total density p_R is equal to the sum of the densities p_I and p_{II} in the principal and additional valleys, and is independent of pressure. Expressing the densities p_i in terms of the corresponding SH oscillation periods, we obtain

$$p_R = a_I (\Delta_3^I)^{-3/2} + a_{II} (\Delta_3^{II})^{-3/2}, \quad (4)$$

where a_I and a_{II} are coefficients that depend on the shapes of the energy valleys [see (6) below]. Figure 4 shows the experimental dependence of $(1/\Delta_3^{II})^{3/2}$ on $(1/\Delta_3^I)^{3/2}$ for sample No. 6p at different pressures. It is well approximated by a straight line. It follows from Fig. 4 that $a_I/a_{II} = 0.16$. Substitution of this ratio in (4) yields at $p_R = 1.2 \times 10^{19} \text{ cm}^{-3}$

$$a_I = 4.7 \cdot 10^{10} \text{ cm}^{-3} \text{ Oe}^{-3/2}, \quad a_{II} = 30 \cdot 10^{10} \text{ cm}^{-3} \text{ Oe}^{-3/2} \quad (5)$$

von Middendorff and Landwehr,³ on the basis of an investigation of the SH oscillations in samples with different hole densities at normal pressure, have proposed a Bi₂Te₃ valence-band model in the form of two six-ellipsoid subbands of the DW type. For such a model

$$a_i = \left(\frac{2em_d}{\hbar cm_s} \right)^{3/2} \frac{1}{3\pi^2}, \quad (6)$$

where m_d is the state-density mass in the subband. Substitution in (6) of the mass values determined for the principal (see Ref. 8) and additional (see Ref. 3) subbands yields values that coincide respectively with a_I and a_{II} from (5). Using $m_3^I/m_3^{II} = 1.8$ we obtain from (5) and (6) the following subband parameters:

$$\begin{aligned} (m_d/m_s)_I &= 4.2; & (m_d/m_s)_{II} &= 14; \\ m_{dII}/m_{dI} &= 1.9. \end{aligned} \quad (7)$$

A large value of $(m_d/m_s)_{II}$ means that the additional ellipsoids should be strongly elongated with a ratio of the length to the transverse dimension not less than 9, as a result of which the length of the ellipsoid for the sample with the maximum density $p_R = 4.4 \times 10^{19} \text{ cm}^{-3}$ (Ref. 3) exceeds the dimensions of the Brillouin zone of Bi₂Te₃. The model of the valence band in the form of two six-ellipsoid subbands³ with large filling of the band is inconsistent. It is possible that the ellipsoidal model of the additional subband is valid in the case of small

filling. On the other hand with increasing density, as proposed earlier,⁹ the additional ellipsoids are deformed and join the principal ones, becoming transformed into hyperboloidal junctions whose lengths, for the same extremal section and volume, can be much less than that of the ellipsoid. We note that if all the subbands are independent, the additional subbands should have a shape more complicated than an ellipsoid.

To determine the baric dependence of the threshold energy we used Eq. (3), in which we substituted the experimental values of the reciprocal periods obtained for sample No. 6p at various pressures. It was assumed that the cyclotron masses m_3^I and m_3^{II} do not change with changing P in first-order approximation. Then E_p decreases linearly with pressure at a rate $\partial E_p/\partial P = -2.7 \times 10^{-6} \text{ eV/bar}$, which is comparable with the pressure dependence of the band gap of Bi₂Te₃.¹⁰ We can thus write in the linear approximation

$$E_p = E_p(0) (1 - P/P^*), \quad (8)$$

where $P^* = 6.8 \text{ kbar}$ is the critical pressure at which the threshold energy is equal to zero. At $P > P^*$ the filling of the valence band starts out from the additional valleys, i.e., an electronic transition characterized by a low pressure is realized in Bi₂Te₃, and when this pressure is exceeded all the holes flow over into the additional valleys, thereby creating conditions favorable for the study of their form with the aid of the SH effect.

Equations (3) and (4) with (8) taken into account from a system of equations with respect to the pressure-dependent variables Δ_3^I and Δ_3^{II} . The results of the solution of this system with the parameters determined above are shown by the solid lines in Fig. 3 for sample No. 6p and in Fig. 2 for sample No. 2p, and by dashed lines for sample No. 2p in Fig. 4. The agreement of the calculated curves with the experimental data for sample No. 2p is somewhat worse than for sample No. 6p. This indicates that the parameters of the system of equations (3) and (4) depend on the degree of filling of the valence band, a fact that can be due, for example, to the non-parabolicity of the principal subband (see the table).

EXPERIMENTAL RESULTS FOR n -Bi₂Te₃ AND THEIR DISCUSSION

A model of the conduction band was proposed earlier,^{1,4} on the basis of an investigation of the SH effect in n -type bismuth telluride, in the form of two subbands: principal (index I), consisting of six ellipsoids, and second (index II), located higher in energy by $E_n = 20-30 \text{ MeV}$. No SH oscillations from the electrons of the upper subband were observed, so that the forms of the additional valleys are unknown. We can write for this model the equation

$$\frac{\hbar^2}{2} (3\pi^2)^{2/3} \left(\frac{n_I^{2/3}}{m_{dI}} - \frac{n_{II}^{2/3}}{m_{dII}} \right) = E_n. \quad (9)$$

Figure 5 shows an experimental plot of $n_{II}^{2/3}$ against $n_I^{2/3}$, which is well approximated by a straight line, and which was obtained for samples with different densities n_R at normal pressure. The electron density n_I in the lower subband was calculated from the period of the SH oscillations at $H \parallel C_3$, using the formula

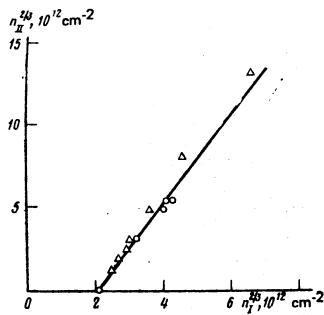


FIG. 5. Plot of $n_{II}^{2/3}$ against $n_I^{2/3}$ obtained for n - Bi_2Te_3 samples with different electron densities $n_R = n_I + n_{II}$ at normal pressure. Circles—present data, triangles—data of Ref. 4.

$$n^* = (3\pi^2)^{-1/3} \frac{2em_d}{\hbar cm_s \Delta_3} \quad (10)$$

with a ratio $(m_d/m_s)_I = 4.14$.¹¹ The density in the upper subband was defined as the difference $n_{II} = n_R - n_I$. The point of intersection of the line with the abscissa axis corresponds to the threshold electron density $n^* = 3 \times 10^{18} \text{ cm}^{-3}$, above which the second subband begins to be filled. The chemical potential ζ^* , which equals E_n at $n_R = n^*$, amounts to $\zeta^* = E_n = 24 \pm 2 \text{ MeV}$ at a state-density mass $m_{dI} = 0.33 m_0$.¹ The slope of the straight line in Fig. 5 yields a ratio $m_{dII}/m_{dI} = 2.6$, which agrees with the earlier data.^{1,2}

We investigated under pressure sample No. 9n with $n_R < n^*$ and sample No. 10n with $n_R > n^*$. Since the Hall coefficient R_3 increased by not more than 10% for either sample, it was assumed that the total electron density n_R is constant. Figure 3 shows the experimental dependence of the reciprocal period $1/\Delta_3^I$ on the pressure for sample No. 10n. The quantity $1/\Delta_3^I$, and consequently also the section of the principal valleys, increases with pressure. Taking into account the results for p - Bi_2Te_3 , we can propose that the gap E_n between the subbands in the conduction band increases under pressure and that the electrons flow over from the second subband to the principal one. Calculation of E_n at various pressures by means of formula (19), using $m_{dII}/m_{dI} = 2.6$, yields a linear increase of the gap at a rate $\partial E_n / \partial P = 1.5 \times 10^{-6} \text{ eV/bar}$. For sample No. 9n ($n_R < n^*$) the periods of the oscillations along the principal

crystallographic directions [see $\Delta_3^I(P)$ on Fig. 2] are practically independent of pressure, thus confirming the assumption that the flow-over plays the principal role in the change of Δ_3^I in n - Bi_2Te_3 at $n_R > n^*$.

Thus, an investigation of the SH effect in Bi_2Te_3 under hydrostatic compression has shown that the relative placement, on the energy scale, of the nonequivalent extrema vary both in the valence band and in the conduction band. In the valence band this leads at $P \approx 7 \text{ kbar}$ to a change of the extremum—to an electronic transition. The transition of Bi_2Te_3 into the metallic state at $P \approx 46 \text{ kbar}$ (Ref. 12) is apparently due to the overlap of the second subband of the valence band and the principal subband of the conduction band. The pressure range 7–40 kbar is therefore of greatest interest for the investigation of the anisotropy of the new absolute extremum of the valence band of Bi_2Te_3 by the SH-oscillation method.

- ¹R. B. Mallinson, J. A. Rayne, and R. W. Ure, *Phys. Rev.* **175**, 1049 (1968).
- ²V. V. Sologub, A. D. Goletskaya, and R. V. Parfen'ev, *Fiz. Tverd. Tela (Leningrad)* **14**, 915 (1972) [*Sov. Phys. Solid State* **14**, 783 (1972)].
- ³A. von Middendorff and G. Landwehr, *Sol. State Comm.* **11**, 203 (1972).
- ⁴B. Schröder, A. von Middendorff, H. Köhler, and G. Landwehr, *Phys. stat. Sol. (b)* **59**, 561 (1973).
- ⁵E. S. Itskevich, *Prib. Tekh. Eksp. No. 4*, 148 (1963).
- ⁶A. A. Averkin and V. N. Bogomolov, *ibid.* No. 6, 224 (1972).
- ⁷J. R. Drabble and R. Wolfe, *Proc. Phys. Soc.* **69B**, 1101 (1956).
- ⁸L. R. Testardi, P. J. Stiles, and E. Burstein, *Sol. State Comm.* **1**, 28 (1963).
- ⁹V. V. Sologub, R. V. Parfen'ev, and A. D. Goletskaya, *Pis'ma Zh. Eksp. Teor. Fiz.* **21**, 711 (1975) [*JETP Lett.* **21**, 337 (1975)].
- ¹⁰A. A. Averkin, O. S. Gryaznov, and Yu. Z. Sanfirov, *Fiz. Tekh. Poluprov.* **10**, 584 (1968) [*Sov. Phys. Semicond.* **10**, 350 (1976)].
- ¹¹R. V. Parfen'ev, V. V. Sologub, and B. M. Gol'tsman, *Fiz. Tverd. Tela (Leningrad)* **10**, 3087 (1968) [*Sov. Phys. Solid State* **10**, 2432 (1969)].
- ¹²E. S. Itskevich, S. V. Popova, and E. Ya. Atabaeva, *Dokl. Akad. Nauk SSSR* **153**, 306 (1963) [*Sov. Phys. Dokl.* **8**, 1086 (1964)].

Translated by J. G. Adashko